ARTICLE NO. 79-0148R

Numerical Simulation of Near Wakes Utilizing a Relaxation Turbulence Model

J. D. Waskiewicz,* J. S. Shang,† and W. L. Hankey‡
Air Force Flight Dynamics Laboratory, Wright-Patterson Air Force Base, Ohio

Numerical solutions of the Navier-Stokes equations are presented for the turbulent supersonic near wake of a two-dimensional wedge/flat-plate model. The turbulent closure is provided by a relaxation eddy viscosity model having its origin in mixing length theory, the velocity defect law, and the classic description of the wake. In the present analysis, further study was made of a composite eddy viscosity model which includes the boundary-layer and wake regions. Although the near-wake region is characterized by strong turbulent inviscid-viscous interaction, results indicate that this complex wake flow can be numerically simulated using a simple relaxation eddy viscosity model.

Nomenclature

C_v = constant volume specific heat
e = specific energy
F,G = vector fluxes in mean flow direction
h = base height of wedge/flat-plate model
k = thermal conductivity
L = reference length
M_∞ = freestream Mach number
p = static pressure
pt = pitot pressure
P_0 = freestream stagnation pressure
Re_∞ = freestream Reynolds number based on reference length
t = time
T = static temperature
u,v = velocity components in Cartesian coordinates
U = vector of conserved properties in mean flow equations
U_{max} = maximum velocity in shock layer
x,y = Cartesian coordinates
δ = boundary-layer thickness
ϵ = eddy viscosity coefficient
ζ = wave direction, $\zeta = y - \tan(\sin^{-1}\frac{1}{M_\infty} + \tan^{-1}\frac{v}{u})x$
η = normalized coordinate measured normal to x axis
κ = stretching parameter for grid generation
μ = molecular viscosity coefficient
ν = kinematic viscosity, μ/ρ
ρ = density
τ = shear stress

Subscripts

i = initial value
TE = trailing-edge value
w = wall value
∞ = freestream value

Introduction

COMPUTATIONAL fluid mechanics has progressed to the stage that both the steady and unsteady transonic flows about an airfoil can be systematically evaluated by numerical procedures.[1-3] However, a common deficiency for most of the calculations is that the numerical results frequently exhibit a significant deviation from experimental measurements[1-3] in the vicinity of the trailing edge. This flowfield is characterized by a strong shock wave/boundary-layer interaction with relatively extensive regions of separated flow. The turbulence model used in the numerical effort was identified as one of the major contributors of the discrepancy.[1] Under certain conditions, periodic motions were also observed. The large-scale, quasiperiodic motion often associated with wakes was also detected in the numerical results for incompressible viscous flows over airfoils.[4,5] This type of fluid motion is caused by periodic shedding of vortices. More recently, the large eddy motion of the organized structure in a wake has been recognized.[6] The present analysis utilizes the Navier-Stokes equations in mass-average variables in an attempt to resolve only the mean characteristics of the steady, supersonic near-wake problem. Even though the present effort concentrates on a specific near-wake problem, numerical solutions can provide valuable insights toward the understanding of the physical processes essential to obtaining a complete description of this phenomenon.

For the purpose of fluid mechanical analysis, wakes may be separated into near-wake, far-wake, and asymptotic-wake regions.[7] The near wake is intimately related to the trailing-edge problem. This problem was analyzed by Goldstein[8] within the framework of boundary-layer theory and more recently by Jobe and Burggraf[9] using an asymptotic expansion scheme based upon the well-known, triple-deck structure[10,11] in which the discontinuity in transverse velocity has been smoothed. Nevertheless, a finer substructure is required to resolve the discontinuous pressure gradients.[9] In the compressible regime, the fluid mechanical phenomena are further complicated by shock wave interactions with the free shear layer.[12-14] For a wake generated by a body with finite transverse dimension, two induced shock wave systems that have been identified are the lip shock,[14] originating at the shoulder due to the rapid overexpansion, and the sequential trailing shock due to the "neck" region.[12,13] Both shock waves are a direct result of strong viscous-inviscid interactions. Because of these interactions, it becomes necessary to use the Navier-Stokes equations to investigate the near-wake problem.

A series of efforts[12,13] has been carried out by Lees and his co-workers in the study of laminar or turbulent wakes through the use of multimoment integral equations. The use of several simplifying approximations has prevented the near-wake problem from being completely resolved.[7] Numerical solutions by means of the Navier-Stokes equations have also

Presented as Paper 79-0148 at the AIAA 17th Aerospace Sciences Meeting, New Orleans, La., Jan. 15-17, 1979; submitted Aug. 30, 1979; revision received Jan. 23, 1980. This paper is declared a work of the U.S. Government and therefore is in the public domain.
Index category: Jets, Wakes, and Viscid-Inviscid Flow Interactions.
*Aerospace Engineer. Member AIAA.
†Aerospace Engineer. Associate Fellow AIAA.
‡Senior Scientist. Associate Fellow AIAA.

been obtained by Roache and Mueller,[15] Allen and Cheng,[16] and Ross and Cheng.[17] In general, the documented results are limited to relatively low Reynolds numbers or an artificial restriction in the viscosity coefficient.[16] The present analysis attempts to investigate the near-wake problem for either laminar or turbulent flows by means of the compressible Navier-Stokes equations. The main emphasis is to delineate the near-wake structure in conjunction with a mixing length turbulence model. The abrupt change in the eddy viscosity coefficient from the boundary layer to the wake is approximated using the concept of a relaxation eddy viscosity model[18] to represent the vastly different length scales in the problem.

In order to test the validity of the numerical procedure, the supersonic near wake of a two-dimensional wedge/flat plate was simulated at a Mach number of 2.25 and Reynolds number of 1.5×10^6 at the trailing edge. Freestream pressure and temperature were 0.2337 atm and 136 K, respectively. Comparisons with experiment include total and static pressure distributions as well as details of the overall flow structure.[19] In particular, the base pressure, recirculation region, and lip and neck shock waves are identified.

Governing Equations

The governing equations of the present analysis are the unsteady compressible Navier-Stokes equations in terms of mass-averaged variables. The adoption of the eddy viscosity coefficient and the turbulent Prandtl number reduces the conservation equations to a form nearly identical for laminar flows. The conservation equation can be written in vector form as follows:

$$\frac{\partial U}{\partial t}+\frac{\partial F}{\partial x}+\frac{\partial G}{\partial y}=0 \tag{1}$$

The vector components are

$$U=\begin{vmatrix}\rho\\ \rho u\\ \rho v\\ \rho e\end{vmatrix}$$

$$F=\begin{vmatrix}\rho u\\ \rho u^2-\sigma_x\\ \rho uv-\tau_{xy}\\ (\rho e-\sigma_x)u-\tau_{xy}v-k\dfrac{\partial T}{\partial x}\end{vmatrix}$$

$$G=\begin{vmatrix}\rho v\\ \rho uv-\tau_{xy}\\ \rho u^2-\sigma_y\\ (\rho e-\sigma_y)v-\tau_{xy}u-k\dfrac{\partial T}{\partial y}\end{vmatrix}$$

where the apparent stress components are given by

$$\sigma_x=-p-\tfrac{2}{3}(\mu+\epsilon)\left(\frac{\partial u}{\partial x}+\frac{\partial v}{\partial y}\right)+2(\mu+\epsilon)\frac{\partial u}{\partial x}$$

$$\sigma_y=-p-\tfrac{2}{3}(\mu+\epsilon)\left(\frac{\partial u}{\partial x}+\frac{\partial v}{\partial y}\right)+2(\mu+\epsilon)\frac{\partial v}{\partial y}$$

$$\tau_{xy}=(\mu+\epsilon)\left(\frac{\partial u}{\partial y}+\frac{\partial v}{\partial x}\right)$$

The mean specific total energy is defined as

$$e=C_vT+(u^2+v^2)/2 \tag{2}$$

Auxiliary relationships needed to complete the system of equations are the equation of state, perfect gas assumption, and Sutherland's viscosity law. Specification of the eddy viscosity model, molecular Prandtl number (0.72), and turbulent Prandtl number (0.9) completes the system of equations.

Boundary Conditions

The system of equations is parabolic in time and elliptic in space, and constitutes an initial value and boundary value problem. The associated initial and boundary conditions (Fig. 1) are prescribed as follows: The initial conditions and upstream boundary conditions are prescribed for all the dependent variables as their unperturbed, freestream values

$$U(0,x,y)=U_\infty \tag{3}$$

The upstream inflow condition is specified as the unperturbed freestream and a well-defined boundary layer.

$$U(t,x_i,y)=U(y) \tag{4}$$

The outflow condition is given at a location far downstream of the trailing edge where the asymptotic free shear layer behavior prevails. A vanishing gradient is an adequate approximation to the physical phenomenon.

$$\partial U/\partial x=0 \tag{5}$$

The outer or far-field conditions for the present analysis are divided into two regions, upstream and downstream of the expansion corner. The former is satisfied by prescribing freestream conditions

$$\lim_{y\to\infty} U=U_\infty \tag{6}$$

The region downstream of the expansion corner is described by a wave boundary condition

$$\partial U/\partial\zeta=0 \tag{7}$$

The near-field conditions at the solid contour satisfy the no-slip condition in velocity components with an adiabatic wall to duplicate the test condition[19]

$$u(t,x,0)=0 \qquad v(t,x,0)=0 \tag{8}$$

$$T(t,x,0)=T_w \text{ (constant)}$$

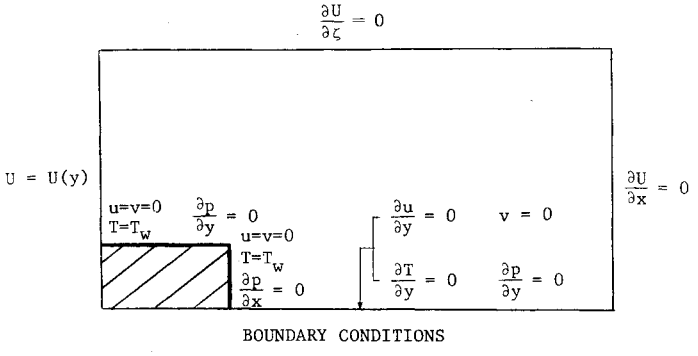

Fig. 1 Computational domain boundary conditions.

The pressure at the solid surface is obtained by assuming that the pressure gradient vanishes in the immediate region of the surface:

$$\frac{\partial p}{\partial y}=0 \tag{9}$$

On the centerline of the wave region, a symmetry condition is imposed.

$$\frac{\partial u}{\partial y}=0 \qquad v=0$$

$$\frac{\partial T}{\partial y}=0 \qquad \frac{\partial p}{\partial y}=0 \tag{10}$$

Eddy Viscosity Model

Turbulent closure was completed by adopting a simple relaxation eddy viscosity model. The basic model has its origin in mixing length theory and the velocity defect law, which is the classic description of the wake formulation. In the boundary layer the two-layer mixing length model of Cebeci and Smith[20] was used. In the wake region the velocity defect law written for the far-wake limit was used.

Boundary Layer

Inner region:

$$\epsilon_i=\rho k_1^2 y^2 D^2 |u_y| \tag{11}$$

where k_1 is the von Kármán constant (0.4) and D is the Van Driest damping factor

$$D=1-\exp[-y(|\tau_w/\rho_w|)^{1/2}/26\nu_w]$$

Outer region:

$$\epsilon_0=k_3\rho U_{\max}\theta_i\gamma \tag{12}$$

where $k_3=0.0168(1.280)=0.0216$; $\gamma=[1+5.5(y/\delta)^6]^{-1}$ (intermittency)

Far Wake

Inner region:

$$\epsilon_i\to\epsilon_0 \tag{13}$$

Outer region:

$$\epsilon_0=k'\rho U_{\max}\theta_i\gamma=\epsilon_{le} \tag{14}$$

where

$$\theta_i=\int_0^\infty\left(1-\frac{u}{U_{\max}}\right)\frac{u}{U_{\max}}\,dy \quad \text{and} \quad k'=0.064$$

k' was determined from empirical correlations.[12,21]

A relaxation model was used to account for the complicated interaction of scaling in spatial response of the turbulent structure to a rapidly changing flowfield. This behavior is substantiated by several research efforts that indicate the Reynolds shear stress remains nearly frozen at its initial value and is convected along streamlines in highly accelerated (or decelerated) flows.[22,23] Measurements[23] also indicate that the Reynolds stress approaches a new equilibrium state exponentially. A reasonable explanation of this phenomenon has been given by Bradshaw.[24] In the present analysis, the history effects are given by the following simple form

$$\frac{\epsilon-\epsilon_{TE}}{\epsilon_{le}-\epsilon_{TE}}=1-\exp\left(-\frac{\Delta x}{\lambda\delta_{TE}}\right) \qquad \text{for} \quad x\geq x_{TE} \tag{15}$$

where ϵ_{TE} is the calculated eddy viscosity coefficient at the trailing edge and ϵ_{le} is the calculated local equilibrium value in the wake. The streamline distance between these two stations is denoted by Δx while δ_{TE} is the boundary-layer thickness at the trailing edge. λ is the relaxation length scale and is given as: $\lambda\simeq 50$.

Computational Grid System

In all calculations a 64×45 computational mesh was employed. Grid spacing in the x direction was uniformly distributed throughout the computational domain with the wake region occupying approximately 75% of the domain. Since a fine mesh spacing is usually required normal to the body for resolution in high gradient areas, a variable distribution of grid points was chosen (see Fig. 2).

For the wedge/flat-plate combination, the most critical area is in the vicinity of the shoulder where the expansion fan, shear layer, lip shock, and trailing shock are predominant features of the flow. To provide adequate resolution for these features in the flow structure, it was necessary to develop an exponentially varying distribution of points with high concentration of grid points adjacent to the shoulder.

In the area of the wake below the shoulder a second exponential grid was used that originated at the shoulder and ended at the wake centerline (see Fig. 2). The finest step was assigned to the shoulder location and has a dimension of 0.59 mm. The physical dimensions of this computational field were 162.4×21.9 mm.

Numerical Procedure

Initially, the present analysis adopted Shang's implicit-explicit numerical scheme[25] to perform the calculations. The advantage this scheme has over MacCormack's strictly explicit method[26] is that the viscous portion of the layer is solved implicitly, thereby easing the restriction on the minimum time step requirement in a fine mesh region. In the outer region where the explicit scheme was used, the relatively large Δy becomes comparable to the Δx step, resulting in much larger time steps.

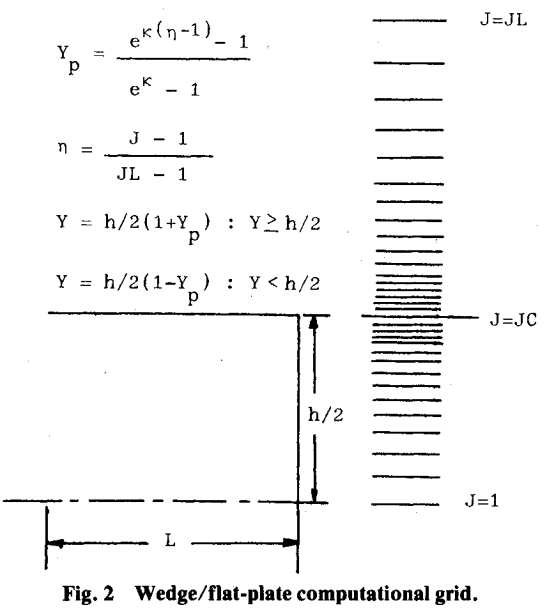

Fig. 2 Wedge/flat-plate computational grid.

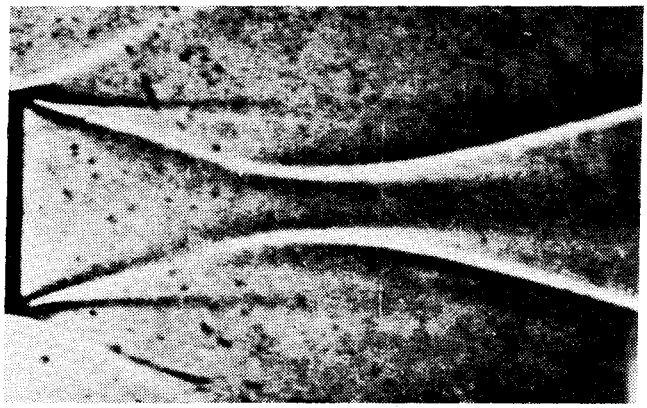

Fig. 3 Shadowgraph of wedge/flat-plate model (Ref. 19).

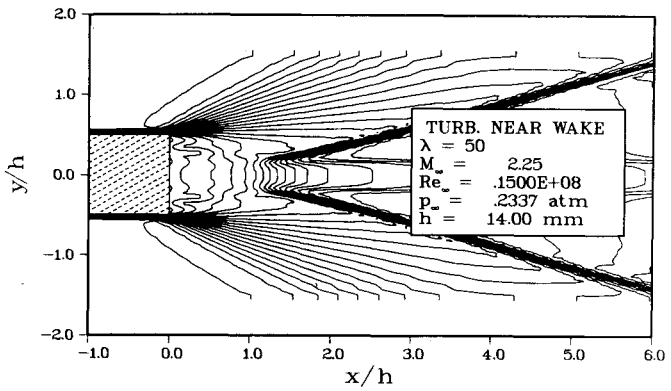

Fig. 4 Density contour map for wedge/flat-plate model.

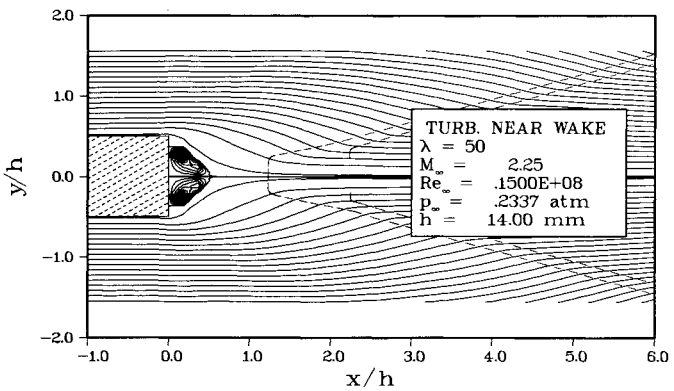

Fig. 5 Streamline map for wedge/flat-plate model.

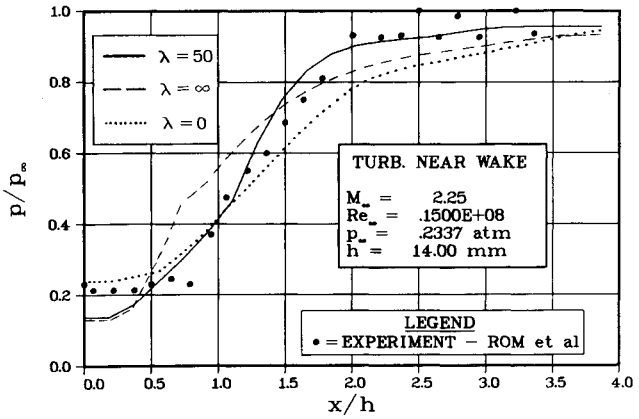

Fig. 6 Comparison of axial pressure distributions for various relaxation length scales.

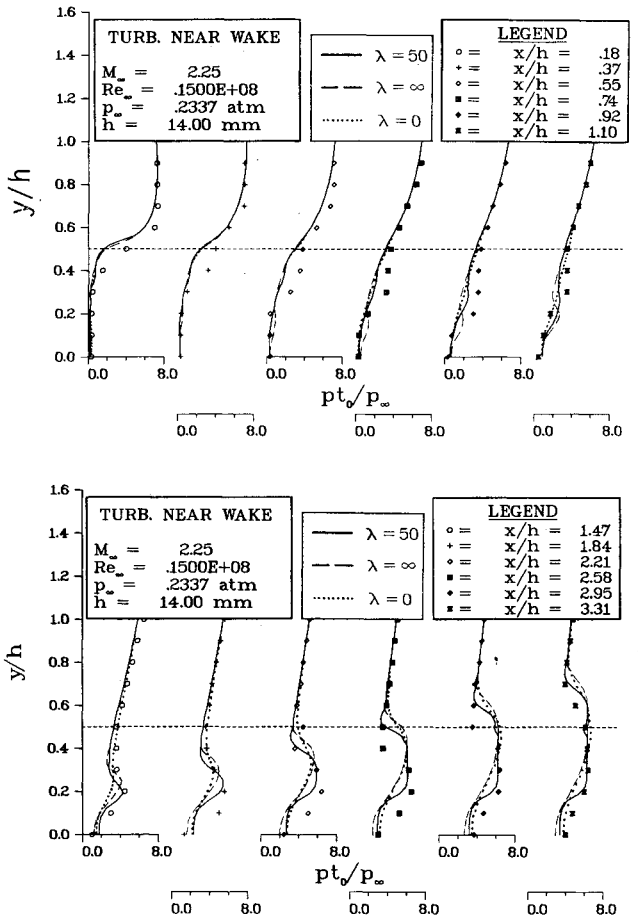

Fig. 7 Comparison of pitot pressure distributions for various relaxation length scales.

The solution scheme was changed to the fully explicit method for two reasons: 1) the implicit technique develops instabilities when used in an area having large normal velocity components, i.e., expansion around the corner; and 2) due to the grid point distribution for this case, the minimum time step requirements were not as rigid, allowing the explicit method to be used without a large increase in computer time.

Calculations were performed on a CDC CYBER 174 digital computer. The rate of data processing was 0.0023 s per grid point for each time step. The evolution of dependent variables was monitored until the consecutive calculations indicated no significant change (0.1%), then the result was considered to be the asymptotic solution.

Results

To verify the computational method in the near-wake region, it was necessary to obtain detailed flowfield data for this area. Although many investigations exist, there are little detailed flowfield data available for turbulent, supersonic near wakes. One of the most complete studies available was performed by Rom et al.[19] on a two-dimensional, wedge/flat-plate model. The experimental data available for the comparison purpose consist of a shadowgraph of the entire flowfield (Fig. 3), the base pressure, and several pitot pressure surveys across the wake region.

In order to simulate the identical conditions of the experimental observation, the numerical procedure started with initial conditions on the flat plate section. Freestream Reynolds number and boundary-layer thickness at the trailing edge were matched to simulate the flowfield over the body. A plot of the density field (Fig. 4) and a streamline map (Fig. 5) were used to identify specific features of the flow. Com-

parisons made with experimental measurements of axial pressure distribution along the wake centerline and pitot pressure surveys of the flowfield are shown in Figs. 6 and 7.

Identifying the relaxation length scale for the turbulence model presented a problem since there was not enough information available concerning the evolution of the eddy viscosity model from the body to the far wake. To determine the effect of this parameter on the flowfield, three different values were tested. The frozen model ($\lambda=\infty$) freezes the eddy viscosity at the upstream value. At the other end of the spectrum is the equilibrium model ($\lambda=0$). This model provides an instantaneous response in the eddy viscosity calculation when the wake is encountered. The last variation ($\lambda=50$) was chosen based upon the results obtained from the frozen and equilibrium cases and studies performed by Alber and Lees.[12] This parametric study not only confirmed the value of the relaxation length scale determined by other investigators, but also provided an understanding for the sensitivity of the flowfield to the eddy viscosity calculation.

Specific features of the flow can be seen from the density field and a streamline map. Although the different relaxation length values produced variations in the static and pitot pressure comparisons, the main features of the flow were not changed. For this reason, only the $\lambda=50$ model will be discussed. Figure 5 is a streamline map of the flowfield. Three features of the flow to be noted are: 1) the turning of the flow through the trailing-edge expansion fan, 2) the pocket of subsonic recirculation near the base, and 3) the recompression through the trailing shock. Tracking of the shear layer from the boundary layer to the wake is also visible in the figure.

Figure 4 is a density contour map of the flowfield showing the leading edge of the expansion fan and the location of the trailing shock. Two other features of the flow which can be observed are the formation of a weak lip shock near the corner and the neck of the trailing shock located approximately one base height downstream of the trailing edge. Figure 3 is a shadowgraph of the near wake taken from the experimental study. A comparison of the density contour map and this photograph indicates that the main features of the flowfield have been predicted by the numerical method, thereby indicating its ability to capture details of the flow structure in the near-wake region.

All comparisons made up to this point have been qualitative with the basic structure of the flow being identified. The quantitative accuracy of the numerical predictions must now be addressed. Available experimental data that can be used for this purpose include static pressure measurements along the wake centerline, base pressure measurements, and pitot pressure surveys at various locations in the wake. It now becomes necessary to discuss differences in the numerical predictions caused by the various relaxation length scales tested.

Figure 6 presents comparisons of the axial static pressure distributions between the experiment and the numerical method for the frozen, equilibrium, and $\lambda=50$ relaxation length scale models. In the far wake, the experimental pressure ratio reaches 0.975 at approximately two base heights downstream of the trailing edge, while the numerical predictions approach this value asymptotically. Both the frozen and equilibrium predictions fail to capture the pressure recovery until nearly four base heights downstream of the trailing edge. In the region less than two base heights from the trailing edge, the frozen model provides the worst agreement with the data. It is clear that the equilibrium model provides better agreement in this area. The $\lambda=50$ model provides the best overall agreement except on the base where the prediction is less than 6% of p_∞ low.

Figure 7 provides pitot pressure comparisons at 12 stations located between 0.1 and 3.5 base heights downstream of the trailing edge for each relaxation length scale model. This figure shows that the frozen model fails to capture the correct location for the recompression shock wave, while the equilibrium model comparisons indicate a failure to predict the correct position of the trailing shock, especially near the neck ($x/h=1.0$). This behavior is attributed to the larger eddy viscosity produced by the equilibrium model in this region. Once again the $\lambda=50$ model provides the best overall agreement. The remaining difference in the numerical ($\lambda=50$) and the experimental data can be attributed to the fact that the numerical method used tends to smear shocks and has difficulty locating weak shocks. In addition, truncation errors and boundary condition approximations also contribute to the error.

Conclusions

The numerical method used in this study reproduces the essential flow features associated with the turbulent, supersonic wake of a wedge/flat-plate model. The relaxation phenomenon has been modeled by adopting an exponential decay of the eddy viscosity with a characteristic length scale. The relaxation eddy viscosity model of Ref. 18 has been combined with the Navier-Stokes equations to form a closed system of equations. Although the model is simple, results demonstrate that it can adequately predict the inviscid-viscous interacting turbulent flow in both the boundary layer and the wake.

For the near-wake region of the model, all of the specific features of the flow have been identified and found to be in good agreement with the experiment. Quantitative comparisons have been made for three relaxation length scales ($\lambda=0$, 50, ∞), with the best agreement found to be for the $\lambda=50$ model.

References

[1] Levy, L.L., "Experimental and Computational Steady and Unsteady Transonic Flows about a Thick Airfoil," *AIAA Journal*, Vol. 16, June 1978, pp. 564-572.

[2] Deiwert, G.S., "Numerical Simulation of High Reynolds Number Transonic Flows," *AIAA Journal*, Vol. 13, Oct. 1975, pp. 1354-1359.

[3] Walitt, L., King, L.S., and Liu, C.Y., "Computation of Viscous Transonic Flow About a Lifting Airfoil," AIAA Paper 77-679, June 1977.

[4] Hodge, J.K. and Stone, A.L., "Numerical Solution for Airfoils Near Stall in Optimized Boundary-Fitted Curvilinear Coordinates," submitted to *AIAA Journal*.

[5] Metha, V.D. and Lavan, Z., "Start Vortex Separation Bubbles and Stall; A Numerical Study of Laminar Unsteady Flow Around an Airfoil," *Journal of Fluid Mechanics*, Vol. 67, 1975, pp. 227-256.

[6] Roshko, A., "Structure of Turbulent Shear Flows: A New Look," Dryden Research Lecture, *AIAA Journal*, Vol. 14, Oct. 1976, pp. 1349-1357.

[7] Murman, E.M., "Experimental Studies of a Laminar Hypersonic Cone Wake," *AIAA Journal*, Vol. 7, Sept. 1969, pp. 1724-1730.

[8] Goldstein, S., "Concerning Some Solutions of the Boundary Layer Equations in Hydrodynamics," *Proceedings of Cambridge Philosophical Society*, Vol. 26, 1970, pp. 1-30.

[9] Jobe, C.E. and Burggraf, O.R., "The Numerical Solution of the Asymptotic Equations of Trailing Edge Flow," *Proceedings of Royal Society, Series A*, Vol. 340, 1974, pp. 91-111.

[10] Stewartson, K., "On the Flow Near the Trailing Edge of a Flat Plate II," *Mathematika*, Vol. 16, 1969, pp. 106-121.

[11] Messiter, A.F., "Boundary Layer Flow Near the Trailing Edge of a Flat Plate," *SIAM Journal of Applied Mathematics*, Vol. 18, 1970, p. 241.

[12] Alber, I.E. and Lees, L., "Integral Theory for Supersonic Turbulent Base Flows," *AIAA Journal*, Vol. 6, July 1968, pp. 1343-1351.

[13] Reeves, B.L. and Lees, L., "Theory of the Laminar Near Wake of Blunt Bodies in Hypersonic Flow," *AIAA Journal* Vol. 3, Nov. 1965, pp. 2061-2074.

[14] Hama, F.R., "Experimental Studies of the Lip Shock," *AIAA Journal*, Vol. 6, Feb. 1968, pp. 212-219.

[15] Roache, P.J. and Mueller, T.J., "Numerical Solutions of Compressible and Incompressible Laminar Separated Flow," *AIAA Journal*, Vol. 8, March 1970, pp. 530-538.

[16] Allen, J.S. and Cheng, S.I., "Numerical Solution of the Compressible Navier-Stokes Equations for the Laminar Near Wake," *Physics of Fluids,* Vol. 13, Jan. 1970, pp. 37-52.

[17] Ross, B.B. and Cheng, S.I., "Finite-Difference Solution of the Laminar Supersonic Near Wake—A Posteriori Error Study and Physical Discussion," Aerospace Research Lab, Wright-Patterson Air Force Base, Ohio, ARL-TR-74-0121, Oct. 1974.

[18] Shang, J.S. and Hankey, W.L., "Numerical Solution for Supersonic Turbulent Flow Over a Compression Ramp," *AIAA Journal,* Vol. 13, Oct. 1975, pp. 1368-1374.

[19] Rom, J., Kronzon, Y., and Sejiner, A., "The Velocity Pressure and Temperature Distribution in the Turbulent Supersonic Near Wake Behind a 2-D Wedge-Flat Plate Model," *Israel Journal of Technology,* Vol. 6, 1968, pp. 84-94.

[20] Cebeci, T., Smith, A.M.O., and Mosinskis, G., "Calculations of Compressible Adiabatic Turbulent Boundary Layer," *AIAA Journal,* Vol. 8, 1970, pp. 1974-1982.

[21] Townsend, A.A., *The Structure of Turbulent Shear Flow,* Cambridge University Press, Cambridge, 1956, Chap. 7.

[22] Diessler, R.G., "Evolution of a Moderately Short Turbulent Boundary Layer in a Severe Pressure Gradient," *Journal of Fluid Mechanics,* Vol. 64, Part 4, 1974, pp. 763-774.

[23] Narasimha, R. and Prabhu, A., "Equilibrium and Relaxation in Turbulent Wakes," *Journal of Fluid Mechanics,* Vol. 54, Part 1, 1972, pp. 1-17.

[24] Bradshaw, P., "Effects of Streamline Curvature on Turbulent Flow," AGARDograph 169, Aug. 1973.

[25] Shang, J.S., "Implicit-Explicit Method for Solving the Navier-Stokes Equations," *AIAA Journal,* Vol. 16, May 1978, pp. 496-502.

[26] MacCormack, R.W., "Numerical Solutions of the Interaction of a Shock Wave with a Laminar Boundary-Layer," *Lecture Notes in Physics,* Vol. 4, Springer-Verlag, New York, 1971, pp. 151-163.